# Transport of Ozone in the Middle Stratosphere: Evidence for Planetary Wave Breaking

C. B. LEOVY, C-R. SUN, M. H. HITCHMAN AND E. E. REMSBERG[1]

*Department of Atmospheric Sciences, University of Washington, Seattle, WA 98195*

J. M. RUSSELL, III AND L. L. GORDLEY

*NASA Langley Research Center, Hampton, VA 23665*

J. C. GILLE AND L. V. LYJAK

*National Center for Atmospheric Research,[2] Boulder, CO 80303*

(Manuscript received 3 January 1984, in final form 16 October 1984)

ABSTRACT

Data from the Nimbus 7 Limb Infrared Monitor of the Stratosphere (LIMS) for the period 25 October 1978—28 May 1979 are used in a descriptive study of ozone variations in the middle stratosphere. It is shown that the ozone distribution is strongly influenced by irreversible deformation associated with large amplitude planetary-scale waves. This process, which has been described by McIntyre and Palmer as planetary wave breaking, takes place throughout the 3–30 mb layer, and poleward transport of ozone within this layer occurs in narrow tongues drawn out of the tropics and subtropics in association with major and minor warming events. These events complement the zonal mean diabatic circulation in producing significant changes in the total column amount of ozone.

## 1. Introduction

In two recent papers, McIntyre and Palmer (1983, 1984, hereafter MP) called attention to the irreversible deformation of the field of Ertel's potential vorticity that takes place in the middle stratosphere as a result of planetary waves. In a typical sequence of events, the winter polar vortex, viewed on an isentropic surface, deforms as a disturbance of zonal wavenumber 1 amplifies. A band of high potential vorticity air is drawn out of the vortex and stretched westward and equatorward while a complementary band of low vorticity air spirals in toward the pole from the subtropics. This process ultimately produces irreversible mixing of potential vorticity and as it continues, a relatively well mixed region develops in midlatitudes bounded on both its polar and equatorial edges by narrow regions containing strong potential vorticity gradients.

Because these developments appear to be planetary-scale manifestations of the vorticity wave breaking within critical layers described theoretically by Stewartson (1978) and Warn and Warn (1978), MP termed the process "planetary wave breaking," and have used the term "stratospheric surf zone" to refer to the potential vorticity mixing region. This evocative term is meant to describe a region of significant meridional width in which irreversible deformation has proceeded to such an extent that air parcels originating from well-separated locations on either side are almost everywhere found in close proximity to each other. Tracer distributions are not necessarily fully mixed, although they may appear so in a coarse grained view. The calculations of Hsu (1980), though carried out with a low-order spectrally truncated model, provide an approximate picture of this behavior.

Similar irreversible deformation occurs in other meteorological contexts, for example in the occlusion process, and in the development of blocking ridges with "omega" structure. In the latter case, baroclinic zones tend to form both poleward and equatorward of the blocking ridge, while air within the ridge itself tends to have quite uniform properties. A nice illustration of the way in which such irreversible deformation occurs was given many years ago by Welander (1955). What is unique about the middle stratosphere is the planetary scale of the breaking waves; they are zonal wavenumbers 1 and 2. Because of this, the flow is not complicated by other features at comparable scale and the process can be seen in data sets of only moderate horizontal resolution. Features such as the "surf zone" are of hemispheric rather than regional

[1] Permanent affiliation: NASA Langley Research Center, Hampton, Virginia.

[2] The National Center for Atmospheric Research is sponsored by the National Science Foundation.

scale, and comparisons with theoretical and numerical models of vorticity wave breaking can be made relatively easily using global satellite data sets.

Ertel's potential vorticity is quasi-conservative in the middle stratosphere, but meridional gradients are influenced by diabatic and frictional processes acting on a time scale of weeks to months. Qualitatively similar distributions should develop for any other property of the flow for which sources and sinks tend to establish a meridional gradient on time scales moderately longer than the advective time scale. In the middle stratosphere, ozone is such a property.

In this paper, we show that ozone distributions inferred from Nimbus 7 Limb Infrared Monitor of the Stratosphere (LIMS) measurements support the wave breaking picture proposed by MP. These data also make it possible to develop details of that picture. Here we focus on three details: the effects of wave breaking on the ozone distribution and its synoptic evolution; the vertical structure of the associated ozone variations; and the effect of middle stratospheric mixing on seasonal changes in the ozone concentration. The data are also used to illustrate a wave breaking event in the Southern Hemisphere corresponding to a growing planetary wave. Implications of these results for seasonal, hemispheric, and interannual variations of ozone are briefly discussed in the last section.

## 2. Data

Radiance data from LIMS were processed as described by Gille and Russell (1984) to retrieve ozone and temperature profiles. The resulting vertical profiles along orbital tracks have been interpolated to fixed pressure levels (Table 1) and mapped globally in the form of Fourier coefficients at fixed latitudes using a Kalman Filter algorithm (Rodgers, 1976; Kohri, 1981). The coefficients represent the zonal mean and the lowest six zonal harmonics at 4° latitude intervals from 64°S to 84°N. Geopotential heights at the constant pressure surfaces of Table 1 were obtained in the same format by vertical integration of temperature using the height of the 100 mb surface given by the National Meteorological Center (NMC) as a base. The data span the period 25 October 1978 through 28 May 1979. The ozone maps in this paper display ozone distributions on the 10 mb surface, not on an isentropic surface. However, they closely approximate distributions on the 850 K potential temperature surface.

TABLE 1. List of LIMS pressure levels (mb).

| | | | | | |
|---|---|---|---|---|---|
| 100 | 70 | 50 | 30 | 16 | 10 |
| 7.0 | 5.0 | 3.0 | 2.0 | 1.5 | 1.0 |
| 0.7 | 0.5 | 0.4 | 0.2 | 0.1 | 0.05 |

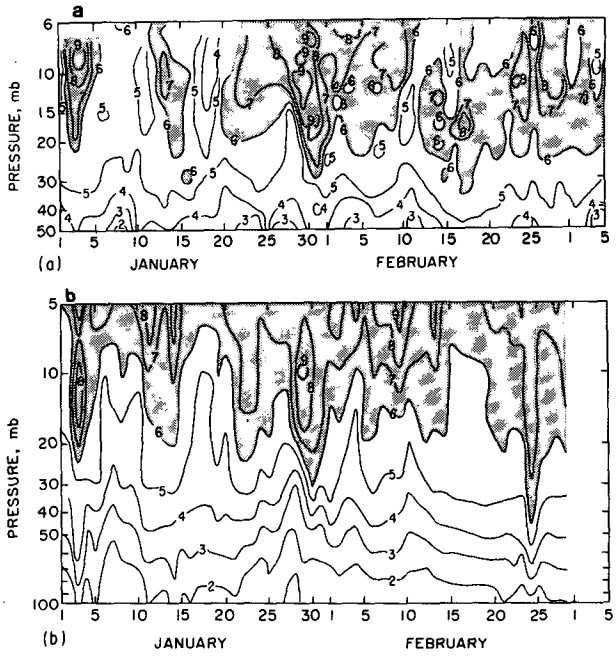


FIG. 1. Time cross sections of ozone concentration (ppmv) at Payerne: (a) Brewer–Mast-sonde ascents published by Dütsch and Braun (1980); (b) interpolated from LIMS.

An overview of the LIMS experiment is given in Gille and Russell (1984). Accuracies, precisions and distributions of systematic error for ozone, temperature, and gradient wind are discussed by Gille *et al.* (1984), Remsberg *et al.* (1984), and Smith and Bailey (1985). In general, neither systematic nor random errors are large enough to affect the results to be discussed below. A characteristic of this data set that proves to be significant is that the data density is greatest at high northern latitudes (excluding the pole itself), so features of relatively small scale can be distinguished there.

## 3. A time series of ozone profiles

A series of daily ozonesonde ascents from Payerne (46.49°N, 6.57°E) utilizing Brewer–Mast sondes has

TABLE 2. LIMS-Hohenpeisenberg ozone correlations (24 soundings).

| Pressure level (mb) | Correlation coefficient | Balloon mean (ppmv) | LIMS mean (ppmv) | Standard deviation | |
|---|---|---|---|---|---|
| | | | | Balloon (ppmv) | LIMS (ppmv) |
| 100 | 0.68 | 1.1 | 1.5 | 0.43 | 0.35 |
| 70 | 0.73 | 2.1 | 2.4 | 0.36 | 0.44 |
| 50 | 0.62 | 3.3 | 3.5 | 0.51 | 0.54 |
| 30 | 0.39 | 5.3 | 4.9 | 0.34 | 0.37 |
| 16 | 0.80 | 6.4 | 6.1 | 1.03 | 1.03 |
| 10 | 0.83 | 6.5 | 6.5 | 1.44 | 0.88 |
| 7 | 0.65 | 6.5 | 6.9 | 1.37 | 0.80 |
| 5 | 0.43 | 7.1 | 7.4 | 1.56 | 0.75 |

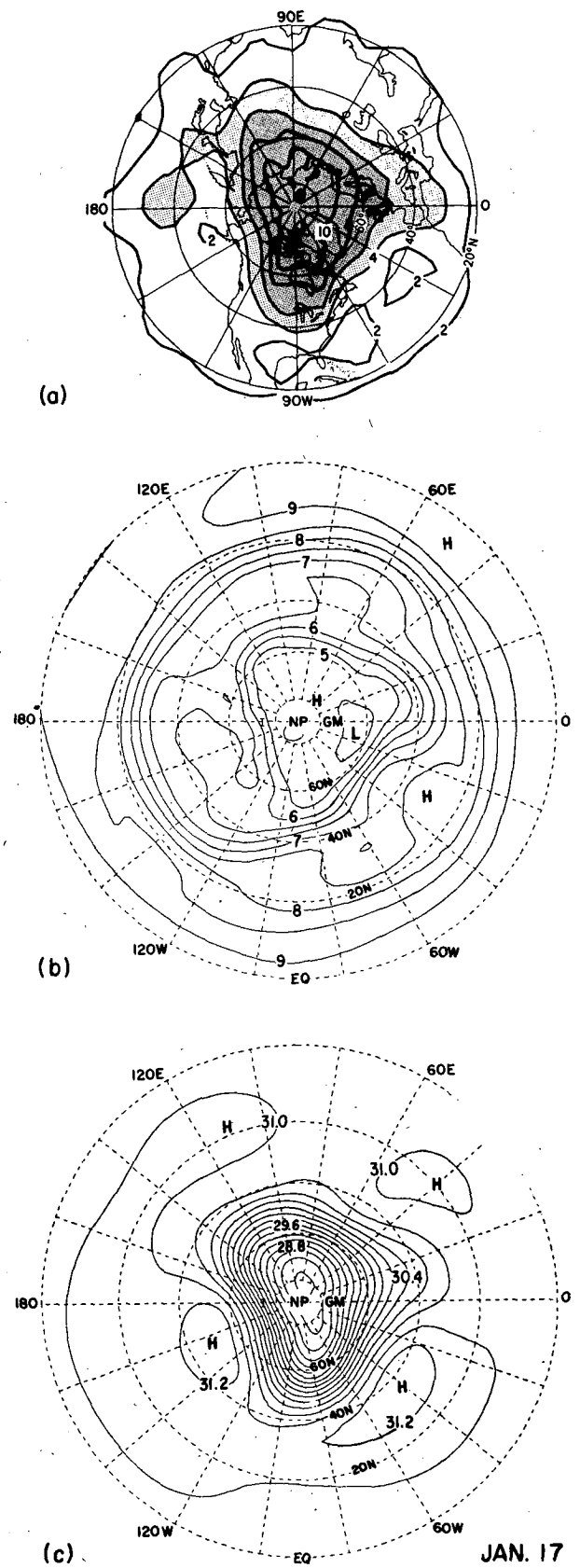


been published by Dütsch and Braun (1980). Since accurate reproduction of profile time series at a fixed location is a severe test of a satellite-borne measurement system, we constructed a comparison series for Payerne using data interpolated spatially from the nearest available LIMS soundings.

The results of this comparison are shown in Fig. 1. It can be seen that the LIMS and *in situ* sections are generally in good agreement. Numerical data were not available to us from Payerne, but data from a more limited series of Brewer–Mast sonde ascents were available from Hohenpeisenberg (47.48°N, 11.01°E), about 330 km from Payerne. The Hohenpeisenberg ascents were carried out approximately three times weekly throughout the winter of 1978/79. Table 2 displays correlations between LIMS and Hohenpeisenberg ascents for the period 1 January–28 February. Except for the 5 mb level where the Hohenpeisenberg series is incomplete and sonde data are less reliable than at lower levels, correlations are moderate to high both above and below 30 mb, but the correlation at 30 mb is low. There are also minima in the standard deviations of LIMS and balloon ozone concentrations at 30 mb.

The reason for the correlation and standard deviation minima at 30 mb can be inferred from Fig. 1. At these middle latitude stations the 30 mb layer separates two regimes. In the lower stratosphere there is a strong mean vertical ozone gradient and fluctuations are characteristically of a 2–3 day period arising from the dominant high-frequency midlatitude tropospheric disturbances. In the middle stratosphere there is a weak mean vertical ozone gradient and ozone fluctuations are dominated by a few transient tongues of high mixing ratio. These fluctuations are due to transient behavior of planetary-scale stratospheric waves. One of these tongues reaches peak intensity near 4 January and another near 30 January. Dütsch and Braun also commented on the regime transition near 30 mb, noting that the intense middle stratospheric ozone tongues, which are well correlated with temperature, could not be readily produced by

FIG. 2. Polar stereographic projections of analyzed Northern Hemisphere fields for 17 January 1979: (a) approximation (of order $Ri^{-1}$) to Ertel's potential vorticity on the 850 K potential temperature surface, from McIntyre and Palmer (1984), (b) 10 mb ozone (ppmv) from LIMS, (c) 10 mb geopotential height from LIMS. In each figure latitude and longitude intervals are 20°, and Greenwich Meridian (GM) 15 is at the right. The 850 K potential temperature surface is close to the 10 mb level in the mean. The quantity corresponding to Ertel's potential vorticity is $(\rho_0/\rho)\eta\partial\theta/\partial z$ where $\rho$ is density, $\eta$ absolute vorticity evaluated using the gradient wind approximation, $\partial\theta/\partial z$ the static stability, and $\rho_0$ is a "standard density" of 1.58 kg m$^{-3}$. It is expressed in units of $10^{-4}$ K m$^{-1}$ s$^{-1}$ (see McIntyre and Palmer, 1984). Differences in small-scale structure (zonal wavenumbers > 6) between potential vorticity and the other fields are due to differences in the data sets and analysis techniques employed. Some of these smaller-scale features may be real.

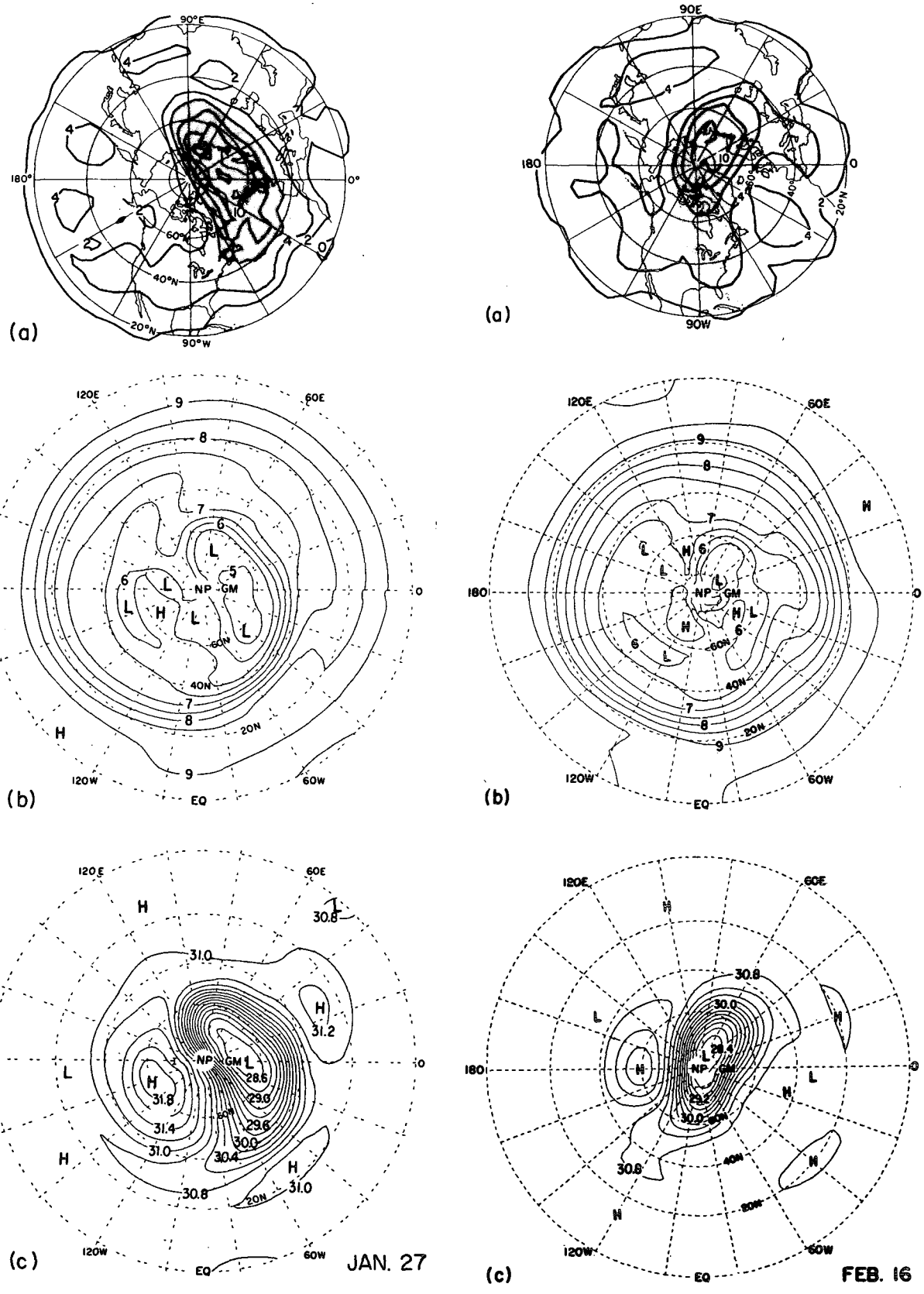


FIG. 3. As in Fig. 2, but for 27 January 1979.

FIG. 4. As in Fig. 2, but for 16 February 1979.

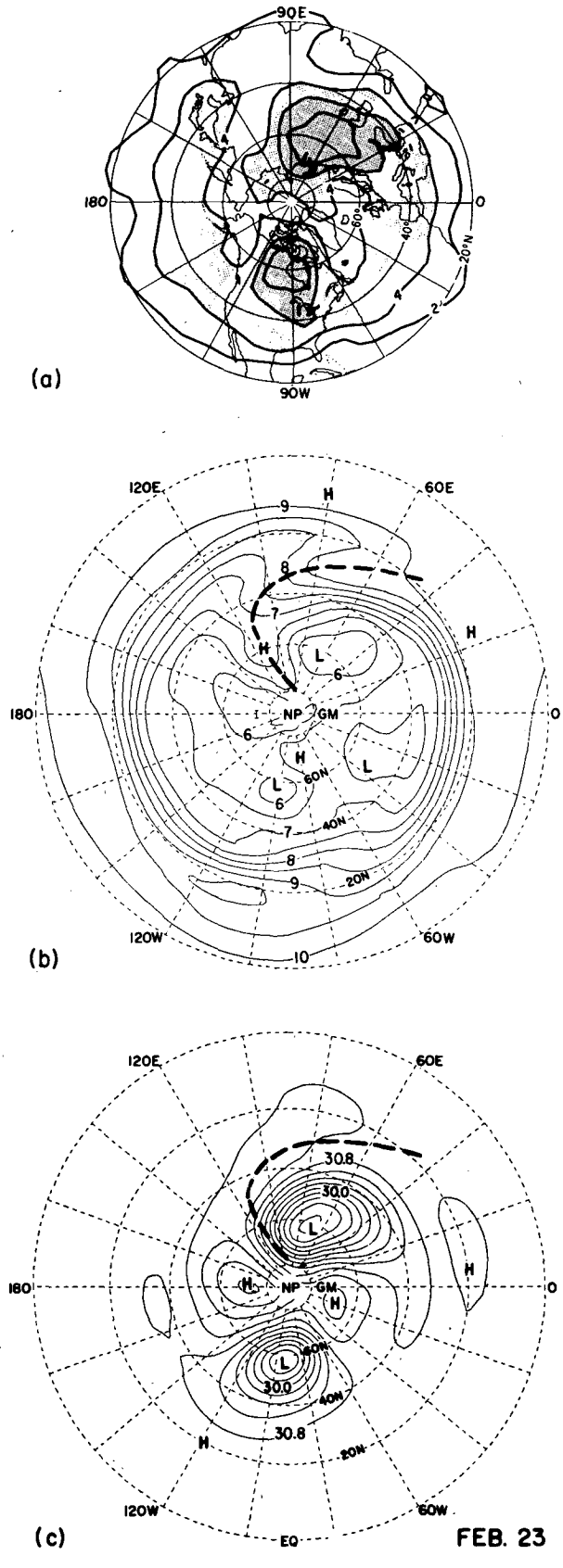


vertical motions in the middle stratospheric region. Such middle latitude ozone tongues, whose representation in the LIMS data is validated by the Payerne and Hohenpeisenberg comparisons, are a focal point of the following sections.

## 4. Ozone and potential vorticity

Figures 2–5 display ozone, potential vorticity, and geopotential height for the four days discussed by MP: 17 and 27 January and 16 and 23 February 1979. There is good qualitative correspondence between ozone and potential vorticity on 17 January with ozone minima and potential vorticity maxima extending equatorward from the polar vortex near 0°E, 100°E and 100°W, strong gradients around the vortex between 50 and 60°N, and a secondary region of strong gradients across the western Pacific between 20 and 30°N. The latter belt of strong gradient is suggested in the potential vorticity map but clearly delineated in the ozone distribution.

The correspondence is even better on 27 January. The vortex has elongated and shifted toward Europe with its edge marked by strong gradients of both ozone and potential vorticity. In both fields, the region of strong gradients spirals clockwise from the edge of the vortex and stretches westward across the Pacific at low latitudes. There is also an indication of a tongue of high ozone and low potential vorticity spiraling inward toward the pole near 50°N, 100°E. Such tongues are prominent in many of the 10 mb ozone maps and will be discussed further in the next section.

The agreement between the ozone and potential vorticity maps is not as good during February, though there are common features: a small vortex elongated and displaced toward Asia on 16 February, a split vortex on 23 February during the major warming, and a secondary region of strong gradient in the 20–30°N latitude belt. Ozone variations during this period will be discussed in detail in the next section. Differences between the ozone and potential vorticity patterns are attributed to differences in the influence of the mean diabatic circulation on mean gradients and to differences in the nonconservative processes affecting their distributions. This will also be discussed further.

## 5. Evolution of circulation and ozone distribution at 10 mb

The time-dependent behavior of ozone at 10 mb in the Northern Hemisphere during the 1978/79 winter provides valuable insight into the mechanism

FIG. 5. As in Fig. 2, but for 23 February 1979. A tongue of ozone-rich air described in the text is indicated by the heavy dashed lines in (b) and (c).

of meridional transport and mixing of ozone and also provides strong support for the "surf-zone" concept of MP. The patterns of ozone behavior can be broadly divided into four periods: a period of weak mixing with incipient breaking waves; a period of prominent wave breaking dominated by the interaction between the Aleutian Anticyclone and low-latitude waves; a period of very large amplitude breaking waves with ozone-rich air streaming into the polar cap (this period includes the major warming of 1979); and a final period of reduced ozone mixing by large scale waves. Each of these periods will now be described in detail.

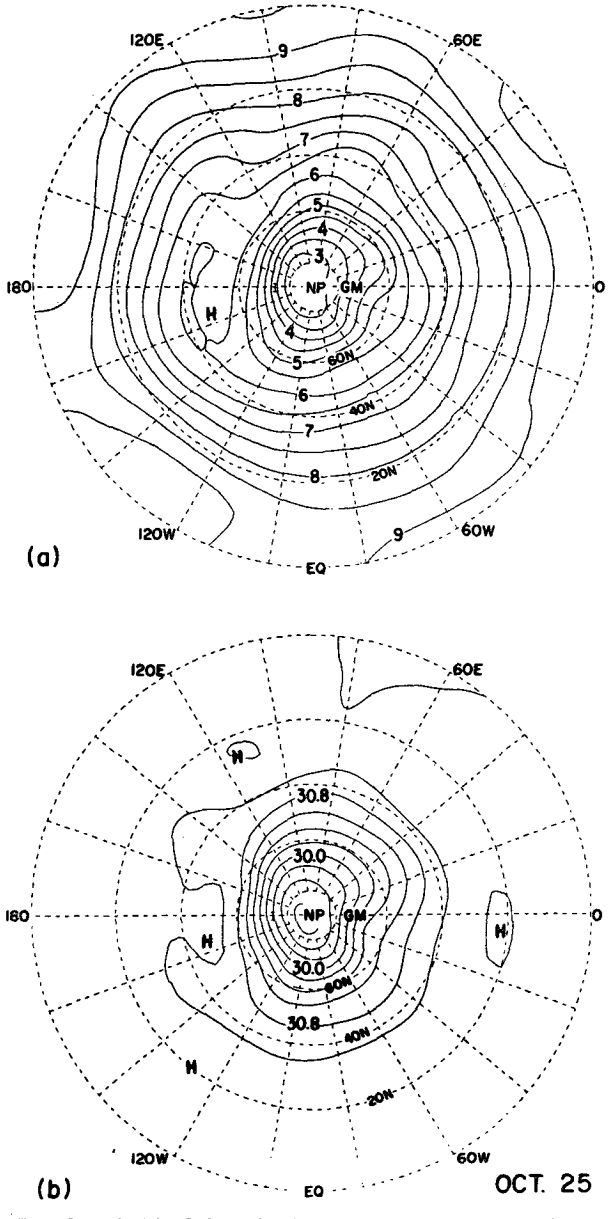


FIG. 6. As in Fig. 2, but 10 mb ozone and geopotential height only for 25 October 1978.

*a. 25 October–29 November: Weak ozone mixing with incipient breaking waves*

At the beginning of the ozone map sequence, 25 October, the 10 mb flow consisted of a nearly symmetric polar vortex together with a nearly symmetric ozone distribution. Meridional gradients of ozone were large and nearly uniform with a deep minimum, an "ozone hole," at the pole with a central value of less than 3 ppmv (Fig. 6). The most significant departure from regularity was a region of weak ozone gradient near 50°N, 170°E which was associated with a weak ridge. Two days later, a wave 2 feature was evident in the middle latitude flow and even more strikingly in the ozone (Fig. 7). The ozone distribution exhibited the weak gradients and northeast–southwest tilting features that are characteristic of the breaking wave model, but only in the 40–60°N belt. This wave 2 feature remained weak and exhibited some amplitude fluctuations, but it could be followed for about 25 days. During that time, it rotated eastward at an average rate of about 13 deg longitude per day. The 40–60°N belt containing these wave 2 ozone features also contained the critical layer in which zonal wind speed and wave phase speed were equal at 10 mb.

Beginning around 17 November, a series of mixing zones, similar to the wave 2 features in the ozone distribution of Fig. 7, began to appear in the low-latitude belt 15–30°N. These features were confined largely to longitudes extending eastward from 140°W to 40°E. Regions of maximum spreading of the ozone contours were generally spaced about 90 deg apart in longitude and were frequently associated with diffluent ridges but features in the low-latitude geopotential height field were generally flat and much less well defined than those in ozone. During this November period, these areas of relatively uniform ozone were again found in the region containing the critical layer at 10 mb, indicating that the apparent quasi-horizontal mixing during this period was due to critical-layer breaking of small amplitude waves.

*b. 30 November–17 January: Prominent wave breaking dominated by the Aleutian anticyclone and low-latitude waves*

During this period, the Aleutian anticyclone began to amplify, and its effects on the ozone distribution became evident. The polar vortex and the associated region of low ozone concentrations were displaced toward the European side of the hemisphere, and a region of strong ozone gradient spiraled westward and outward from the vortex, splitting just downstream from the Aleutian anticyclone, with the low-latitude branch encircling most of the hemisphere between 10 and 20°N (Fig. 8). Between this tropical branch of the spiral and the polar vortex, there was a region of weak ozone gradient, characterized by eastward-pointing tongues of high ozone to the north

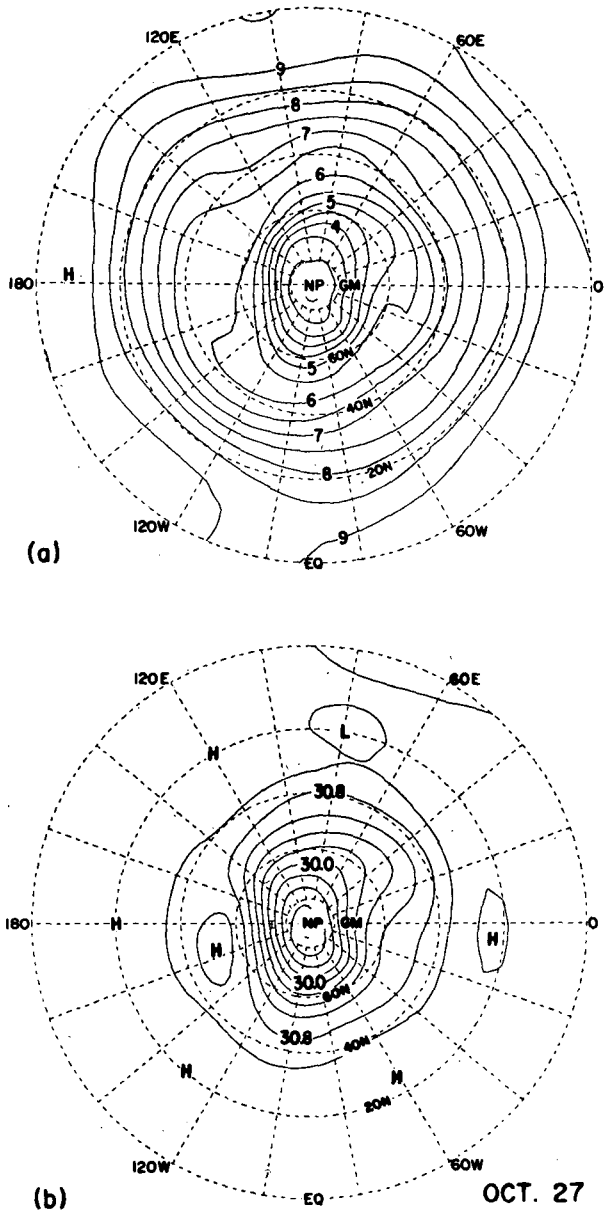


FIG. 7. As in Fig. 6, but for 27 October 1978.

of westward-pointing tongues of low ozone. Figure 8 shows that these tongues were well correlated with the structures of the anticyclones bordering the polar vortex: high ozone tongues appeared near jet entrance regions on the upstream edges of the anticyclones while low ozone tongues originated in the diffluent flow downstream of anticyclonic centers. The 17 January ozone distribution (Fig. 2) falls within this period, but the configuration during late December and early January, like that of Fig. 8, was more striking and more typical. The occurrence of a relatively flat ozone field between regions of strong ozone gradient at both lower and higher latitudes, as well as the structure of the ozone tongues, are consistent with the wave breaking model.

*c. 18 January–5 March: Large amplitude breaking waves with ozone-rich air streaming across the polar cap*

Prior to 18 January, tongues of ozone-rich air developed intermittently and wrapped around the vortex at moderately high latitudes. An example of such a tongue is shown in Fig. 8, extending from 20°N, 0°E to about 35°N, 120°E (heavy dashed line). Two similar ozone-rich tongues acting to replace

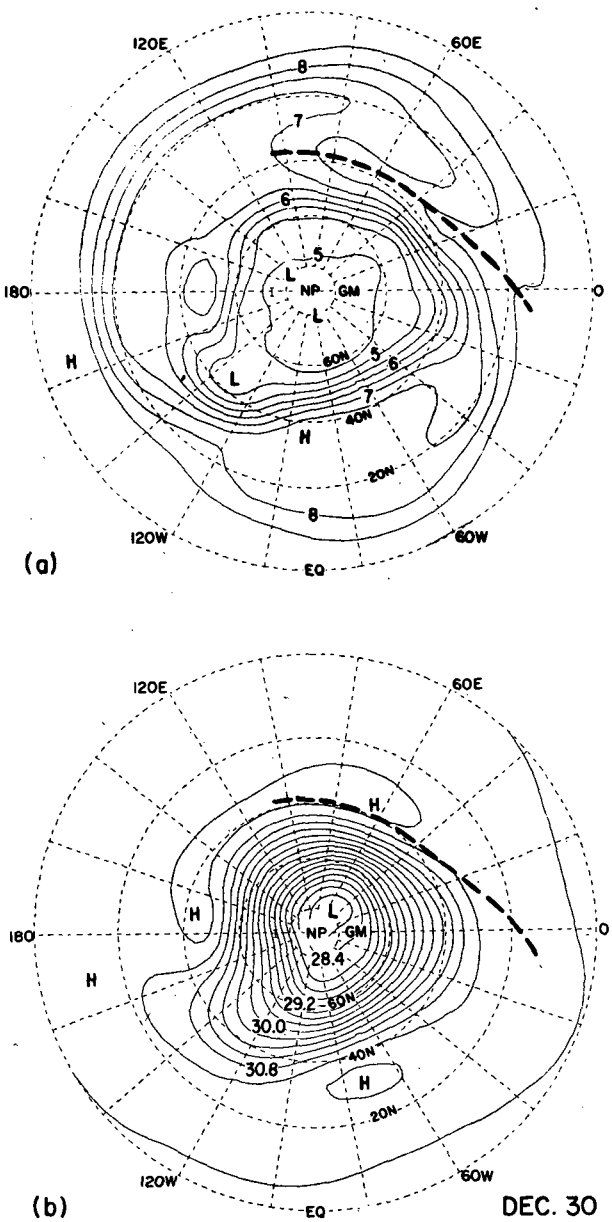


FIG. 8. As in Fig. 6, but for 30 December 1978.

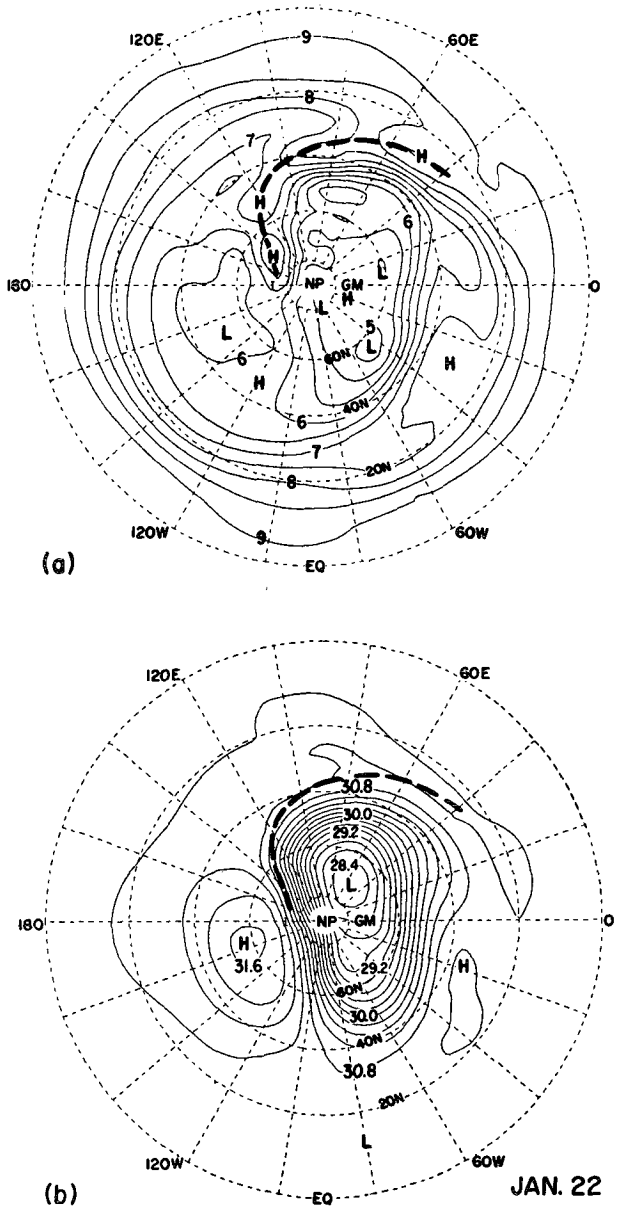


FIG. 9. As in Fig. 6, but for 22 January 1979. The axis of the tongue of ozone-rich air described in the text is marked by heavy dashed curves.

air from the edge of the polar vortex were responsible for the middle stratospheric ozone maxima observed near the beginning and end of January at Payerne (Fig. 1). However, beginning about 18 January, the vortex began to move farther from the pole on the European side of the hemisphere, a process which could also be described as a strong amplification of zonal wavenumber 1 (Smith, 1983). A significant feature of this event was the development for the first time of an ozone-rich tongue extending from the tropics into the interior of the polar cap region. In Fig. 9, this tongue can be traced from near 20°N, 40°E eastward to 70°N, 140°W. By 2 February, this ozone tongue had subsided (Fig. 10), but it had produced a long-lasting splitting of the pool of ozone-poor air with one pocket remaining over Siberia within the vortex and another weaker pocket drifting westward just south of the center of the Aleutian anticyclone where it remained throughout February.

A second surge of ozone into the polar cap region began on 3 February and reached peak intensity on 6 February, when an ozone tongue could be traced eastward from near 20°N, 40°W to 80°N, 150°W (Fig. 11). At this time, the polar region had two distinct ozone minima, one in the vortex near 0°E

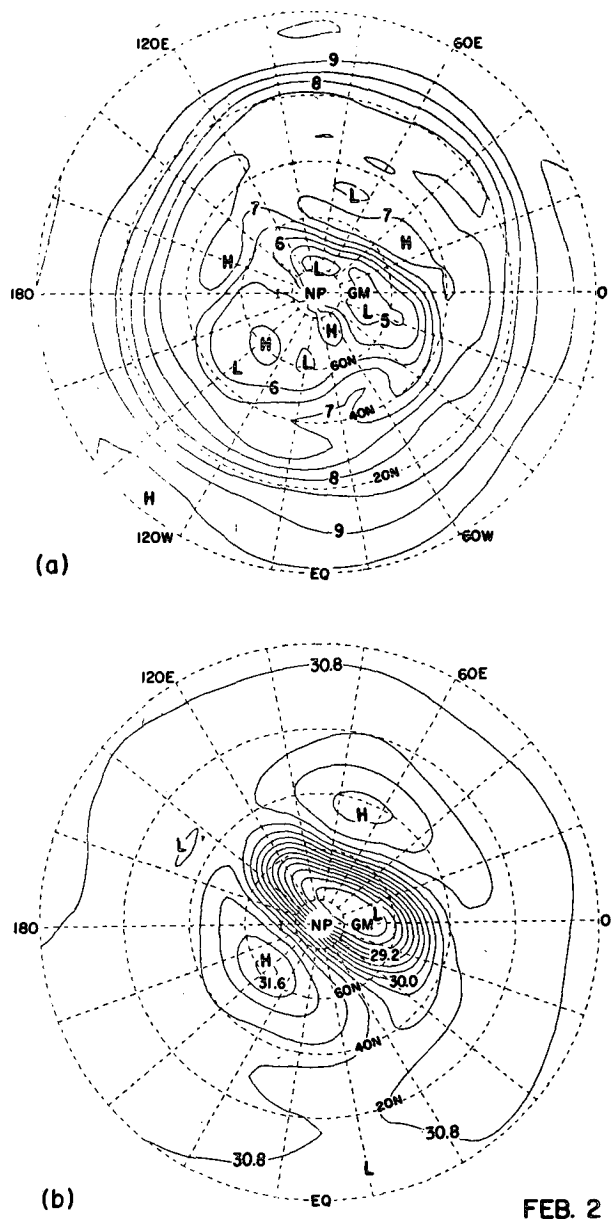


FIG. 10. As in Fig. 9, but for 2 February 1979.

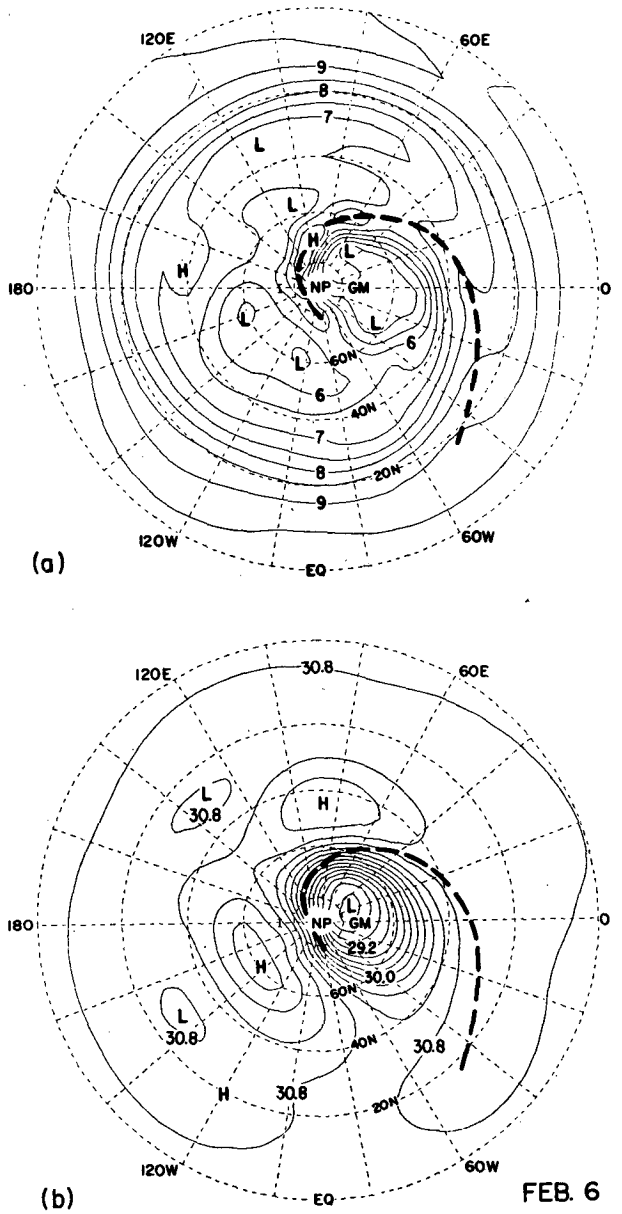


FIG. 11. As in Fig. 9, but for 6 February 1979.

and one in the anticyclone near 140°W; the major stratospheric warming had not yet begun. By 13 February this second ozone surge had subsided, or at least its extension into the tropics had been cut off, but by 20 February a third surge had begun and had reached peak intensity by 24 February, during the development of the major warming at 10 mb. This surge was associated with the splitting of the vortex, or wave 2 amplification, that characterized the warming event (Butchart *et al.*, 1982), but at this time only the larger and more intense branch of the vortex, that on the Asian side, was drawing ozone-rich air into polar regions (Fig. 5). A few days later the main injection of ozone-rich air over Asia had subsided, but a weaker tongue of ozone had developed on the North American side in association with the secondary lobe of the vortex (Fig. 12).

It is interesting that ozone-rich air, and presumably other tracers, penetrated from the tropics into the polar regions in several distinct surges. Inspection of Figs. 9–12 and Fig. 5 gives the impression, reinforced by closer inspection of the entire map series, that these surges were correlated with fairly subtle changes in size and/or shape of the polar vortex. When the vortex was large enough or extended far enough southward that tropical air could be drawn around

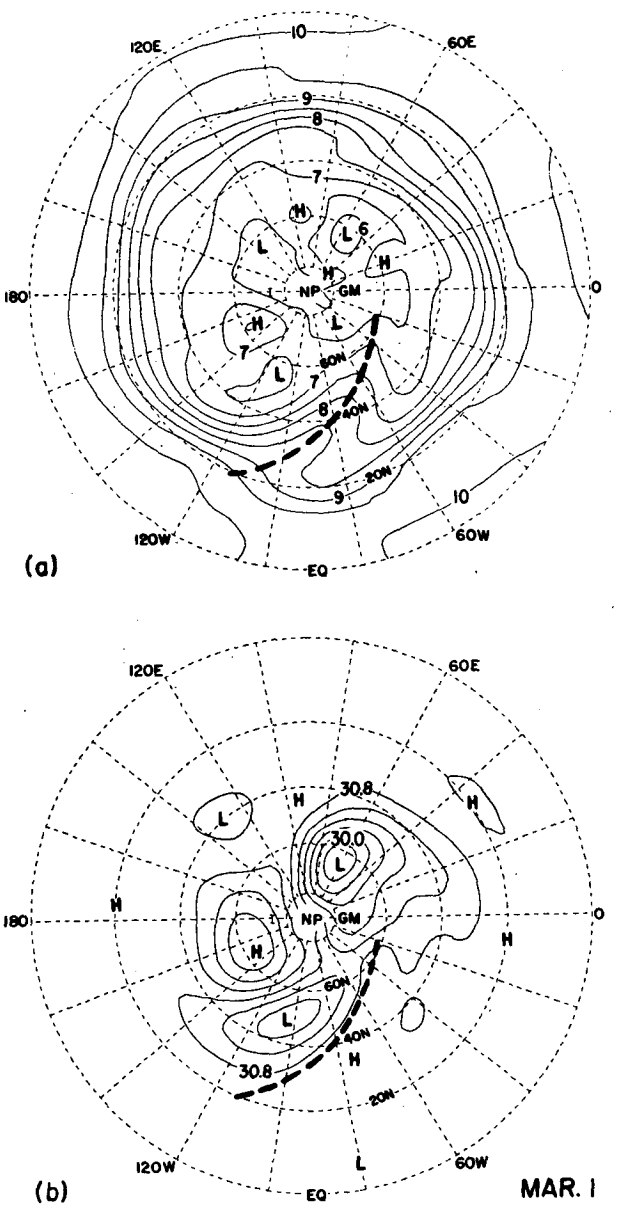


FIG. 12. As in Fig. 9, but for 1 March 1979. Compare with Fig. 5.

its periphery, surges of ozone-rich air from the tropics into the polar cap zone took place. Whenever the vortex edge retreated poleward, the tropical source of the ozone surges was cut off. During the period from late January through February 1979, these equatorward advances and retreats of the vortex edge appeared to occur in a quasi-periodic fashion. Only the last of these events, in which the polar vortex split into two distinct lobes, was associated with a major warming.

### *d. 6 March–28 May 1979: Reduced mixing by large-scale waves*

After the major warming, the ozone field at 10 mb, which was by then rather flat, showed little evidence for lateral mixing by large-scale waves. What mixing activity there was occurred early in the period and in the low latitudes and it was suggestive of weak wave breaking in the vicinity of the critical layer for stationary or slowly-propagating waves. No major surges of ozone-rich air into high latitudes were observed and, with the return of summer to the polar cap region, the ozone distribution began to take on a more "photochemical" appearance with uniform gradients and reformation of a well-defined minimum near the pole.

## 6. Vertical structure of ozone gradient regions

We have identified regions of strong gradients of ozone and potential vorticity on both polar and equatorial edges of the stratospheric surf zones. In order to further delineate the structure of this phenomenon, two vertical cross sections of ozone derived from vertical profiles along orbital tracks close to 0°E are shown in Fig. 13 for two days in late January. The cross sections pass close to Payerne and correspond to the onset and the peak phases of the middle stratosphere ozone surge of late January depicted in Fig. 1. These ozone changes in the 26–30 January period were associated with a temporary poleward retreat of the edge of the vortex in this longitude belt with the largest increase exceeding 3.5 ppmv near 10 mb and 52°N.

The region of strong ozone gradient extended from approximately 30 to 3 mb and near 48°N it tilted poleward with a mean slope of about 1:100 on 26 January, decreasing to about 1:300 on 30 January. From the Payerne and Hohenpeisenberg time series, it appears that the lower boundary is determined by a transition to a region below, dominated by tropospheric waves of relatively high frequency and small zonal wavelength. The zonal mean horizontal gradient of ozone also reverses near 30 mb. Below 30 mb, photochemistry plays almost no direct part in controlling the ozone concentration. The upper boundary of this layer may mark the transition to the regime in which the photochemical time scale is shorter than the transport time scale, so that transport has little influence on the distribution above this level. The slopes shown in Fig. 13 are typical of those in other cross sections we have examined.

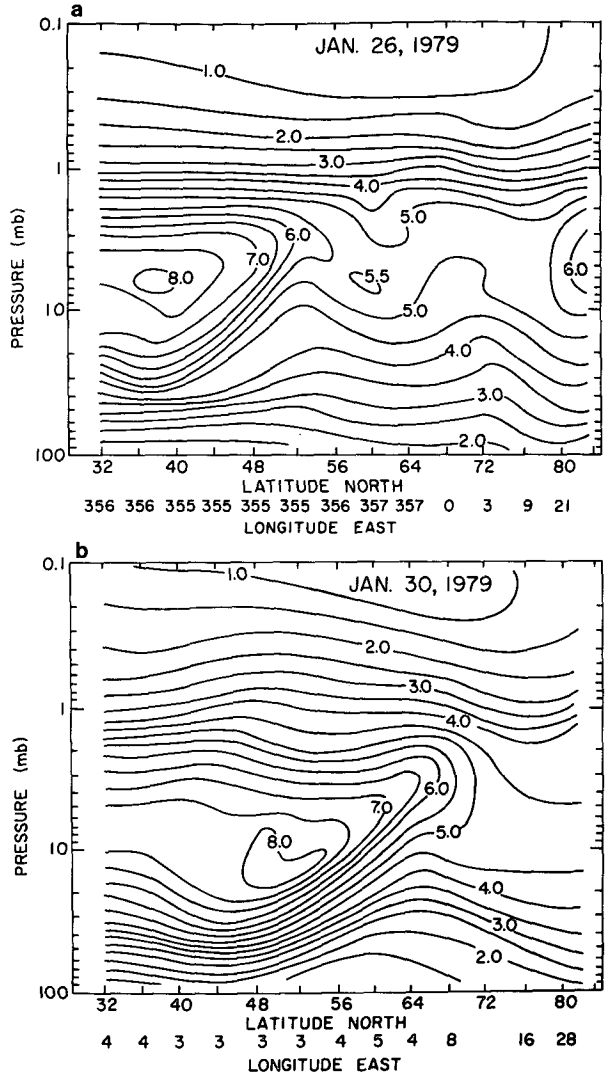


FIG. 13. Meridional cross sections of ozone concentration (ppmv) derived from orbital data approximately along longitude 0°E: (a) 26 January 1979; (b) 30 January 1979.

## 7. A Southern Hemisphere example

Figures 14–16 illustrate stages at one-week intervals in the evolution of a slowly-amplifying wave in the Southern Hemisphere, including the associated changes in the ozone distribution. On 13 May, a series of weak troughs and ridges perturbed the zonal flow south of about 20°S with wavenumber 2 slightly stronger than any of the other components. Along the equatorward edge of the westerlies, the strongest ridge was located near 36°S, 30°E, and the ozone distribution in this area was beginning to deform with a tongue of ozone-rich air protruding southeast-

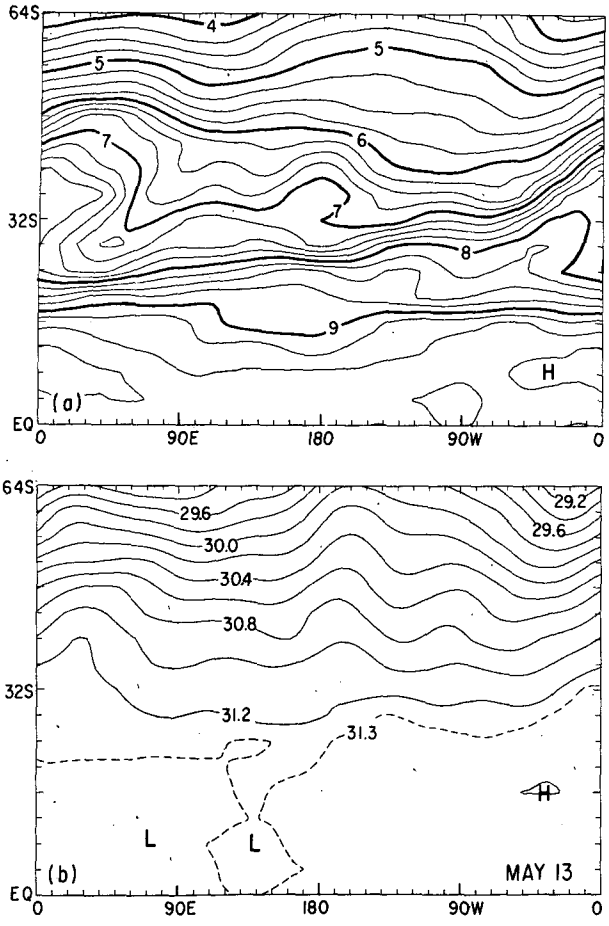


FIG. 14. Southern Hemisphere fields at 10 mb for 13 May 1979: (a) ozone (ppmv); (b) geopotential height. The fields are shown as if seen from below: south is at the top and east is at the right.

ward to the south of a northwestward protruding tongue of ozone-poor air. There was also a hint of a similar pattern near 34°S, 180°E. Both of these features occurred where the mean westerlies were weak, so that they were within or near the critical layer for this slowly eastward-propagating wave field. As a consequence of wave breaking activity in these two regions, a band of enhanced ozone gradient was beginning to form along an arc extending eastward around the earth from 20°S, 0°E to about 40°S, 0°W (Fig. 14).

Over the following two weeks, the wave 2 pattern slowly amplified and rotated eastward at an average rate of about 7 deg longitude per day. By 26 May, the weaker of the two ozone mixing regions noted on the 13 May map had acquired the characteristic structure of a large-amplitude breaking wave centered near 32°S, 90°W (Fig. 16). A sharp concentration gradient zone had developed along the trailing edge of this wave with the characteristic tongues of ozone-rich air and ozone-poor air ahead of (northeast) and behind (southwest) the zone. Such details of the structure as the pocket of ozone-poor air at 28°S, 115°W persisted on the maps for several days and were probably real. This particular feature appeared to have been swept in from higher latitudes and trapped in the propagating wave.

Meridional cross sections through the region of strong ozone gradient (not shown) revealed a sloping structure similar to that in Fig. 13, with slope gradually decreasing from the longitude of the crest of the amplifying ridge to that of the following trough.

## 8. Seasonal changes in the ozone distribution

It is well known that the total column amount of ozone changes in response to major and minor stratospheric warmings (e.g., Ghazi, 1974). In the preceding sections, we have shown that ozone penetrates the polar cap region during warmings in narrow tongues which form in response to the shifting or splitting of the polar vortex away from the polar cap region. From another point of view, these tongues can be regarded as characteristic features accompanying the formation of broad mixing zones which

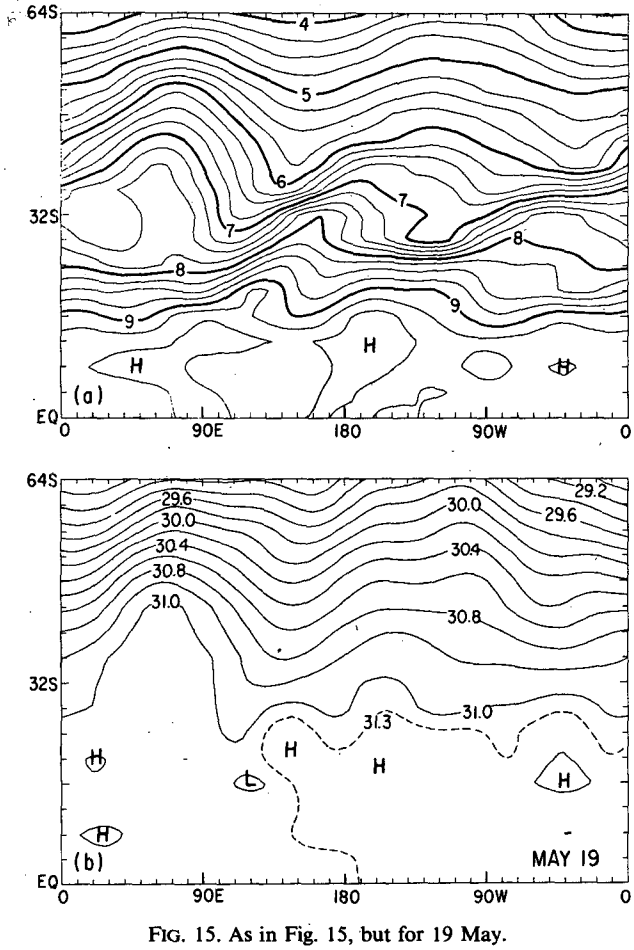


FIG. 15. As in Fig. 15, but for 19 May.

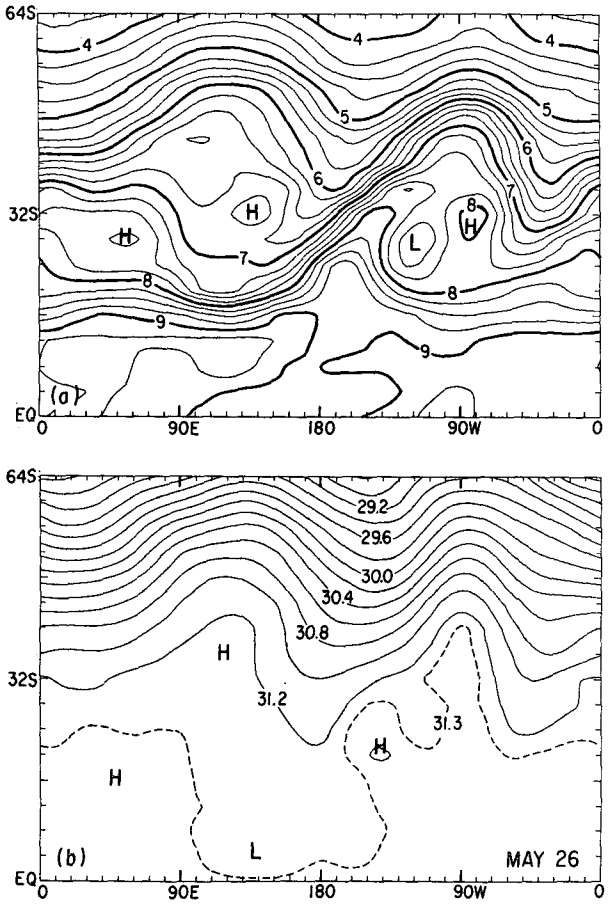


FIG. 16. As in Fig. 15, but for 26 May.

develop in connection with the amplification and breaking of planetary waves. We now examine the relationship between these patterns of mixing in the middle stratosphere and the patterns of change in the ozone column.

Figure 17 shows the change in the ozone column above 30 mb over the intensely active period from the first half of January to the first half of March. The filling of the ozone hole produced an increase in ozone column over the polar cap of up to 50 Dobson units (DU). There was a belt of minimum increases or small reductions in the ozone column around the 30–50°N zone, suggesting that the added polar cap ozone may have been drawn in part from lower latitudes. The changes over this period amounted to a net increase in the vertically-integrated ozone above 30 mb over the Northern Hemisphere. This increase in the hemispherically-integrated ozone came about because ozone transported to the polar region is protected from photochemical destruction while ozone removed from low latitudes is photochemically restored.

The region above 30 mb was chosen for this evaluation because of the indication from Figs. 1 and 13 that 30 mb forms the approximate lower boundary of the region under the direct influence of transport by breaking waves of middle stratospheric scale. The pattern of vertically-integrated ozone change exhibits a polar maximum similar to that of the seasonal changes in total ozone above the ground, and the change above 30 mb at the pole shown in Fig. 17 was about one-third that of the total column. On the other hand, at midlatitudes (30–60°N), changes in the ozone column above 30 mb were much smaller than changes in the total column. Therefore, total ozone changes above 30 mb shown in Fig. 17 represent less than 20% of the change in total ozone burden north of 40°N over the same period (e.g., Dütsch, 1971). However, the 30 mb column change underestimates the influence of middle stratospheric waves on total ozone. Figs. 1 and 13 show that during major ozone surges in the middle stratosphere, despite the tendency for the surges to concentrate in the 3–30 mb layer, increased ozone concentrations did extend below 30 mb. Middle stratospheric ozone surges have an even greater effect in the north polar lower stratosphere. This is illustrated in Fig. 18, which shows large increases in ozone concentration in the 30–100 mb layer at northern polar latitudes following the minor warming of late January and the major warming of late February.

Figure 18 also depicts the changes in zonal mean ozone concentrations along potential temperature $\theta$ surfaces. In isentropic coordinates, the zonal mean ozone mixing ratio is described by

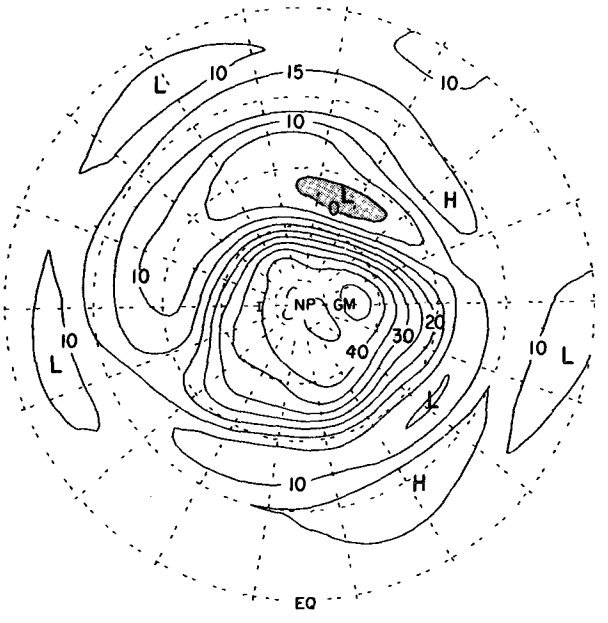


FIG. 17. Change in ozone column above the 30 mb level between the 14-day intervals 1–14 January and 1–14 March 1979. Units are Dobson Units (DU). Map projection as in Fig. 2.

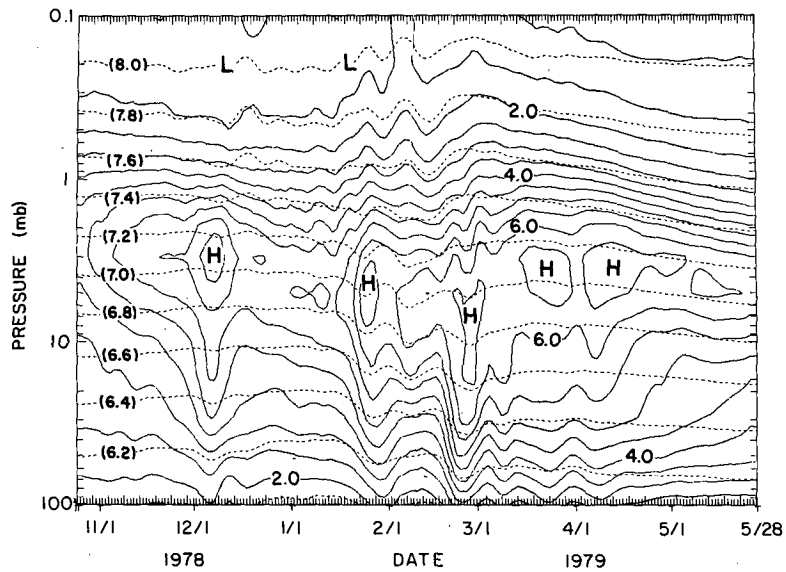


FIG. 18. Time–height cross section of ozone concentration (ppmv) averaged over the latitude belt 76–84°N for the period 25 October 1978 through 28 May 1979. Dashed lines are isentropes, with the values of ln $\theta$ indicated.

$$\frac{\partial \bar{\mu}}{\partial t} + \bar{v}\frac{\partial \bar{\mu}}{\partial y} + \bar{\dot{\theta}}\frac{\partial \bar{\mu}}{\partial \theta} = E + P, \tag{1}$$

where $\bar{v}$ is the mean meridional velocity, $\bar{\dot{\theta}}$ is the diabatic rate of change of $\theta$ (in the zonal mean), and $E$ and $P$ represent the contributions due to eddies and photochemistry respectively (Tung, 1982). The time and meridional derivatives are to be evaluated on isentropic surfaces. During winter in the polar cap zone both $\bar{v}(\partial\bar{\mu}/\partial y)$ and $P$ can be neglected, reducing this equation to

$$\frac{\partial \bar{\mu}}{\partial t} = -\bar{\dot{\theta}}\frac{\partial \bar{\mu}}{\partial \theta} + E. \tag{2}$$

Below about 2 mb during early winter, the ozone changes took place as steady cross-isentropic (downward) displacement of constant mixing ratio surfaces punctuated during early December and after mid-January by rapid fluctuations. The steady displacement component decreased downward and was quite consistent with changes expected from the second term of Eq. (2) for winter diabatic cooling rates in this region. From the mean slopes of the $\mu$-surfaces in Fig. 18, we estimate cooling rates of about 1.3 K day$^{-1}$ at 10 mb and 0.3 K day$^{-1}$ at 50 mb during November through January, values that are quite consistent with calculated cooling rates (e.g., Dickinson, 1984). Therefore we attribute this component of the ozone change to the zonal mean diabatic circulation.

In Fig. 18, rapid fluctuation in ozone mixing ratio during early December was due to a temporary displacement of the main vortex away from the pole in association with amplification of the Aleutian anticyclone. The rapid and more permanent ozone increases below 2 mb after mid-January corresponded with the minor and major warming events. The associated rates of change of ozone mixing ratio were much too large to be due to diabatic cross-isentropic transport, and we attribute the large changes after mid-January to large-scale eddy transport that was predominantly along isentropic surfaces and largely irreversible.

This figure also suggests a cause for the differences between the patterns of ozone and potential vorticity that were observed at the 10 mb level (or on the 850 K potential temperature surface), especially in the region of the polar vortex. In this region, the diabatic circulation advects downward larger values of both potential vorticity and ozone. This tends to fill in the deep polar ozone hole but intensify the polar vortex, and it is consistent with differences in the seasonal trends in the ozone and potential vorticity distributions shown in Figs. 2–5.

Potential vorticity and ozone are also affected in different ways by nonconservative sources and sinks. The advective ozone changes in the polar cap zone are not reversed by photochemistry while those outside of the zone in the middle stratosphere are slowly reversed. The patterns of ozone change shown in Fig. 17 suggest that this effect may be important above 30 mb on the seasonal time scale. It may also account for the persistence of low ozone values in polar latitudes but outside of the main vortex, as shown in Figs. 3, 4, 10 and 11.

The significance of the horizontal gradient of rates of photochemical processes was recognized by Hart-

mann and Garcia (1979). However, the mechanism of poleward transport identified here differs from that of Hartmann and Garcia in that it does not require correlations between meridional velocity and ozone arising from photochemically-produced phase shifts. Instead, the net transport occurs because of wave breaking, a highly nonlinear process. The Hartmann–Garcia mechanism does effect ozone transport (Gille *et al.*, 1980), but only where transport and photochemical time scales are comparable. Since this occurs at a higher altitude where absolute ozone concentrations are much lower and where photochemistry acts rapidly to oppose changes due to transport, wave breaking is a far more effective mechanism for producing changes in the ozone column.

## 9. Discussion

We have attempted to show that the concept of wave breaking provides a useful framework for describing the distribution and transport of ozone in the middle stratosphere (30–3 mb), and that quasi-horizontal transport in wave breaking events, together with the diabatic mean meridional circulation, contributes significantly to seasonal changes in the total vertically-integrated ozone amount. The wave breaking signature in the ozone distribution first appears in association with small-amplitude waves near the critical line, but its latitudinal extent increases with increasing wave amplitude and in the Northern Hemisphere it spreads into the polar region during major and minor warmings. The notions of wave transience and dissipation, which are important in the design of two-dimensional models are, like the wave breaking concept, aspects of Lagrangian transport theory. Wave breaking is an inherently transient process. Such models attempt to account for tracer transport by transient waves, as well as dissipative waves and the diabatic mean circulation (e.g., Rood and Schoeberl, 1983).

The concept of wave breaking provides a quite general view of the eddy transport and serves to focus attention on the conservative behavior of advecting tracers in fully nonlinear flow. For large-amplitude waves and in critical layers for waves of any amplitude, the advective process is always irreversably transient as a result of the continuing deformation and associated stretching of advected fields to smaller scales. Some of the features of breaking waves and the associated mixing are reproducible with low-order spectrally-truncated models such as that of Hsu (1980); indeed, Hsu's model calculations show features quite similar to those in Figs. 6–12. But, because of the restricted freedom of these models, tracer transport tends to occur in large blobs rather than narrow tongues, and transient motions in the absence of explicit or implicit dissipation are reversible. In addition, because of the truncation, potential vorticity is not generally conserved in these models. These differences are illustrated in a recent detailed comparison of wave behaviors in fully nonlinear and in low-order spectrally-truncated models (Haynes, 1983).

Because of the low longitudinal resolution of the LIMS data (and also possibly because of the noise level of the ozone retrievals), we cannot definitively describe the evolution of small-scale features. Nevertheless, at the scale that is accessible (zonal wavenumbers $\leqslant 6$), the breaking wave model seems to apply well. In any case, the transport events associated with major and minor warmings will have to be faithfully represented in two-dimensional models if these models are to simulate stratospheric perturbations adequately.

These results have interesting implications for the interannual and interhemispheric variations in the behavior of the ozone column. They suggest that the effectiveness of the annual filling of the ozone hole and the corresponding increase in the north polar ozone column depends on both the frequency and intensity of injection of ozone tongues from the tropics to the pole which in turn depend on the number, intensity, and duration of warmings each winter. In the Southern Hemisphere, the late winter peak ozone column occurs in subpolar rather than polar latitudes. We speculate that this is due to the persistence of the vortex over the pole throughout the winter, so that the ozone tongues associated with the Southern Hemisphere surf zone cannot reach the pole. Of course there is a final warming in southern spring when the vortex moves off the pole, but the vortex may be too weak, too small, and too short-lived at this point to effectively tap the ozone reservoir at lower latitudes. Rood (1983) has made a similar point.

Several of the questions raised in this initial descriptive study can probably be addressed in further studies using the existing data. These studies include trajectory calculations allowing for nonconservative processes to clarify the relationships between potential vorticity, potential temperature, and ozone; they also include more detailed studies of the influence of breaking planetary waves on the total ozone budget. Answers to questions about interannual variability of the polar winter regions, particularly the south polar winter, must await the advent of observational systems capable of mapping the ozone distribution in these regions.

*Acknowledgments.* We are indebted to M. E. McIntyre, T. N. Palmer, P. H. Haynes, S. Solomon, M. Salby, N. Butchart, M. R. Schoeberl, R. J. Reed, R. B. Rood, and J. R. Holton for helpful discussions and suggestions. E.E.R. participated in this research while at the University of Washington under support from a Floyd L. Thompson Fellowship and Award. Support for this research was provided by the National

Aeronautics and Space Administration under Grants NAGW-471 and W-15439.

## REFERENCES


Butchart, N., S. A. Clough, T. N. Palmer and P. J. Trevelyan, 1982: Simulations of an observed stratospheric warming with quasi-geostrophic refractive index as a model diagnostic. *Quart. J. Roy. Meteor. Soc.*, **108,** 475–502.

Dickinson, R. E., 1984: Infrared radiative cooling in the mesosphere and lower thermosphere. *J. Atmos. Terr. Phys.* (in press.)

Dütsch, H. U., 1971: Photochemistry of atmospheric ozone. *Advances in Geophysics,* Vol. 15, Academic Press, 219–322.

——, and W. Braun, 1980: Daily ozone soundings during two winter months including a sudden stratospheric warming. *Geophys. Res. Lett.*, **7,** 785–788.

Ghazi, A., 1974: Nimbus 4 observations of changes in total ozone and stratospheric temperatures during 1970–71. *J. Geophys. Res.*, **81,** 5365–5373.

Gille, J. C., and J. M. Russell III, 1984: The limb infrared monitor of the stratosphere (LIMS): An overview of the experiment and its results. *J. Geophys. Res.*, **89,** 5125–5140.

——, P. L. Bailey and J. M. Russell III, 1980: Temperature and composition measurements from LRIR and LIMS experiments on Nimbus 6 and 7. *Philos. Trans. Roy. Soc. London,* **296,** 205–218.

——, and Collaborators, 1984: Validation of temperature retrievals obtained by the Limb Infrared Monitor of the Stratosphere (LIMS) experiment on Nimbus 7. *J. Geophys. Res.*, **89,** 5147–5160.

Haynes, P. H., 1983: Non-linear Rossby wave critical layers in the stratosphere. Ph.D. thesis, Cambridge University, 340 pp.

Hartmann, D. L., and R. R. Garcia, 1979: A mechanistic model of ozone transport by planetary waves in the stratosphere. *J. Atmos. Sci.*, **36,** 350–364.

Hsu, C-P. F., 1980: Air parcel motions during a numerically simulated sudden stratospheric warming. *J. Atmos. Sci.*, **37,** 2768–2792.

Kohri, W. J., 1981: LRIR observations of the structure and propagation of stationary planetary waves in the Northern Hemisphere during December 1975. NCAR Cooperative Ph.D. thesis, Drexel University, 312 pp. [NTIS PB82156639.]

McIntyre, M. P., and T. N. Palmer, 1983: Breaking planetary waves in the stratosphere. *Nature,* **305,** 593–600.

——, and ——, 1984: The 'surf zone' in the stratosphere. *J. Atmos. Terr. Phys.*, **46,** 825–850.

Remsberg, E. E., J. M. Russell III, J. C. Gille, L. L. Gordley, P. L. Bailey, W. G. Planet and J. E. Harries, 1984: The validation of Nimbus 7 LIMS measurements of ozone. *J. Geophys. Res.*, **89,** 5161–5178.

Rodgers, C. D., 1976: Retrieval of atmospheric temperature and composition from remote measurements of thermal radiation. *Rev. Geophys. Space Phys.*, **14,** 609–624.

Rood, R. B., 1983: Transport and seasonal variation of ozone. *Pure Appl. Geophys.*, **121,** No. 5, (in press).

——, and M. R. Schoeberl, 1983: Ozone transport by diabatic and planetary wave circulations on a $\beta$-plane. *J. Geophys. Res.*, **88,** 8491–8504.

Smith, A. K., 1983: Observation of wave–wave interactions in the stratosphere. *J. Atmos. Sci.*, **40,** 2484–2496.

——, and P. L. Bailey, 1985: Comparison of horizontal winds from the LIMS satellite instrument with rocket measurements. *J. Geophys. Res.* (in press).

Stewartson, K., 1978: The evolution of the critical layer of a Rossby wave. *Geophys. Astrophys. Fluid Dyn.*, **9,** 185–200.

Tung, K. K., 1982: On the two-dimensional transport of stratospheric species in isentropic coordinates. *J. Atmos. Sci.*, **39,** 2330–2355.

Warn, T., and H. Warn, 1978: The evolution of a nonlinear Rossby wave critical layer. *Stud. Appl. Math.*, **59,** 37–71.

Welander, P., 1955: Studies in the general development of motion in a two-dimensional ideal fluid. *Tellus,* **7,** 141–156.